Electric aerosol particle counting and size distribution measuring system for the 0.015 to 1 μ size range[1]

By KENNETH T. WHITBY and WILLIAM E. CLARK, *Mechanical Engineering Department, University of Minnesota, Minneapolis, Minnesota, U.S.A.*

(Manuscript received December 16, 1965)

ABSTRACT

An electrical particle counter and size analyzer system having the following characteristics has been described.

(1) Sizing range from 0.015 to 1.2 μ.

(2) Classification range from 0.015 to 0.6 μ at 28 l/m aerosol sampling rate.

(3) A unique unipolar diffusion charger that is stable, controllable and capable of near optimum charging performance.

(4) A versatile mobility analyzer capable of discrete classification of particles with mobilities from 0.01 to 0.0002 (cm/sec)/(volt/cm) at aerosol flow rates up to 57 l/m. This analyzer is unique in using a filter located at the aft end of the current collector. This separation of the collecting electrode and the current collector permits the use of collector voltages up to 30 KV while maintaining background currents below 10^{-14} amp.

(5) Although the instrument described here is only semi-automatic, a completely automatic version of the EPC is entirely practical. An automatic EPC used together with an automatic CN and optical counter would permit continuous automatic size distribution measurement over the size range from 0.01 to 10 μ.

Automatic aerosol counting and particle sizing instruments using light scattering principles that are usable in the 0.3 to 10 μ size range are now available (ZINKY, 1962; THOMAS *et al.*, 1960; RANDALL, *et al.*, 1965; and WHITBY & VOMELA, 1965). However, there are currently no equivalent instruments available for the rapid *in situ* sizing and counting of aerosols smaller than 0.3 μ. Although automatic nuclei counters such as the General Electric instrument (SKALA, 1963) are available, these merely give the total particle count larger than some size in the vicinity of 20 Å, and can provide only very limited data on aerosol size distribution.

A study of the problem of rapid sizing and classification of aerosols in the size range below 0.3 μ by our laboratory several years ago suggested that an instrument based on electrical charging and subsequent electric mobility analysis might be feasible. This approach is an old one having been suggested by ROHMAN (1923) more than 40 years ago and having been studied by many investigators since.

[1] This research conducted under Division of Air Pollution, Bureau of State Services, Public Health Service Research Grant No. AP 00136–04.

The principle of this method of sizing and classification is to first charge the aerosol so that the number of charges carried by the different sized particles is of such magnitude that the electrical mobility is a monotonically decreasing or increasing function over the size range of interest and, then, to measure the electrical mobility. Mobility analyzers used by the various investigators have varied with respect to internal geometry, whether the aerosol was introduced across the whole space between the condenser electrodes or as a thin filament in a clean air sheath. A variety of methods for sensing the collection or deflection of the aerosol has also been used.

A study of the previous work suggested that the three major obstacles to the successful design of a practical instrument would be:

1. Design of a stable reproducible charger;
2. Design of a mobility analyzer capable of operating at a large aerosol flow rate while collecting particles having mobilities as small as 0.0002 cm/sec per volt/cm; and
3. Selection of a simple and reliable sensing method.

This paper describes the work that was done to solve the above problems and describes the final instrument.

Some representative data obtained with the electrical particle counter (EPC) used together with the Royco optical particle counter and the General Electric nuclei counter (CNC) as a complete particle sizing and counting system are also presented.

Nomenclature

$\bar{c}$ = mean molecular velocity
C = Cunningham correction
D_i = ion diffusion coefficient, cm^2/sec
D_p = particle diameter, microns or cm
D_{pi} = characteristic particle size in interval, cm or μ
e = 4.8×10^{-10} stat coul or base of natural log
E = electric field, volts/cm or stat volts/cm
f = fraction charged
F_c = (See equation 6)
I = current, amperes
k = Boltzmann's constant
K = analyzer efficiency factor (see Fig. 6)
L = charger length, cm
n_p = no. of unit charges per particle
N = ion density, no./cm^3
N_0 = initial ion density
N_p = particle concentration, no./cm^3
N_{p0} = initial particle concentration, no./cm^3
Q_a = mobility analyzer aerosol air flow, cm^3/sec.
Q_c = mobility analyzer clean air flow, cm^3/sec.
Q_i = ion source strength, stat coul/sec
Q_t = mobility analyzer total air flow, cm^3/sec
r_1 = collector radius, cm
r_2 = mobility analyzer tube radius, cm
r_w = charging chamber wall radius, cm
Re = Reynolds number
t = time, sec
T = absolute temperature, °K
v = flow velocity, cm/sec
V = collector voltage, statvolts or volts
$\bar{x}$ = arithmetic mean distance of deposition, cm
Z_i = small ion mobility, (cm/sec)/(stat volt/cm)
Z_p = electrical particle mobility, (cm/sec)/ (volt/cm) or (cm/sec)/(stat volt/cm)
β = Bricard combination coef. (see equation 3)
$\varkappa$ = $4\pi e Z_i$
λ = mean free path, cm
μ_g = gas viscosity, poise
σ_g = geometric standard deviation

Theory and description of the electrical particle counter

A schematic of the system is shown in Fig. 1 and a photograph in Fig. 2. The basic operation is as follows: Entering aerosol is given a unipolar negative charge by a special diffusion charger. It then passes through an aerosol flow meter to the mobility analyzer where it is introduced as a thin annular cylinder around a core of clean air. The charged aerosol is then drawn inward by the positive potential on the collector rod. If the collector is operated at a constant potential, the aerosol is classified along the rod according to electrical mobility. If the collector voltage is varied in a systematic manner, all particles having a mobility less than a given value will miss the end of the collector rod and be collected by the current collecting filter. The number-particle size distribution curve of the aerosol may be calculated from the filter-current versus collector-rod voltage curve.

Although the normal mode of operation is to use the charger to impart a unipolar negative charge to the aerosol, the natural positive or negative charge on an aerosol can be easily obtained by measuring the filter collector current as the (+) or (−) potential on the collector rod is varied.

Since the instrument is intended for use in classifying and sizing of normal atmospheric

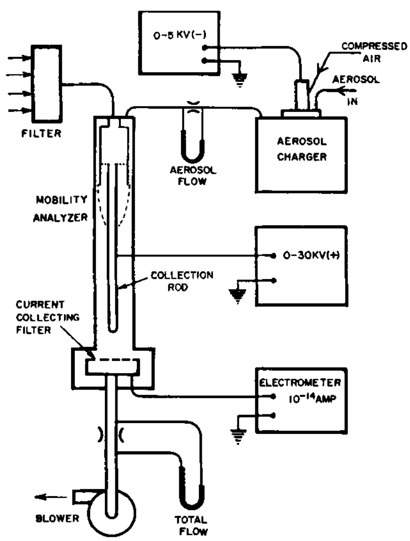

FIG. 1. Schematic of the electrical particle counter system.

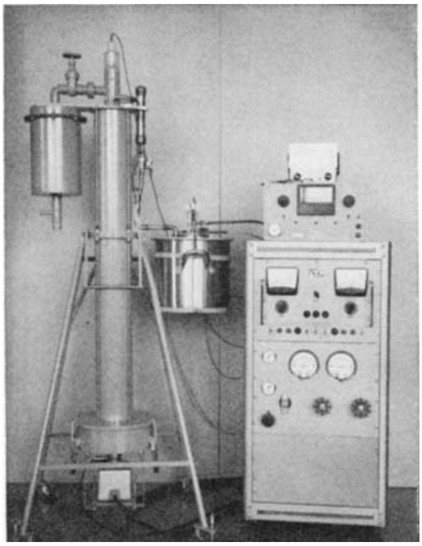

FIG. 2. The electrical counter system showing the mobility analyzer, charger, and electric and flow instrumentation.

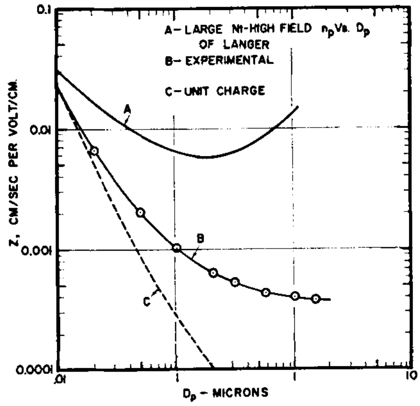

FIG. 3. Mobility versus particle size for field and diffusion charging.

aerosol concentrations, relatively large aerosol flow rates were required. Following are the performance specifications of the final instrument.

1. Aerosol flows up to 70 liter/min.
2. Mobility range from 0.01 to 0.0002 (cm/sec)/(volt/cm).
3. Particle sizing and classification from 0.015 to 1.0 μ at 30 l/m and 0.015 to 0.5 μ at 70 l/m aerosol flow.
4. Ten percent mobility resolution.
5. Discrete separation of mobility.
6. Ability to electrically measure the mobility distribution of bipolar aerosols.

All of the work reported here has been done using a vibrating reed electrometer as the sensor. Typical currents are 7×10^{-12} amp when sampling a normal urban atmospheric aerosol at 30 l/m. Some experiments using a General Electric automatic condensation nuclei counter as the particle sensor have also been made.

Aerosol charger

Unipolar charging of small aerosol particles is readily accomplished by exposing them to small ions of one sign under the proper conditions. The aerosol particles may be exposed to the ions in the absence of an electric field (pure diffusion charging) or in a strong electric field (field charging).

However, the relationship between particle charge and particle size and, consequently, the relationship of mobility to size, is different for the two modes of charging. For both diffusion and field charging, particles larger than about 0.05 μ are multiply charged, so that there is some size at which the electrical mobility, Z_p, is a minimum. It can be seen from Fig. 3 that the minimum Z_p occurs at about 0.2 μ for strong field charging (Curve A) and at about 3 μ for the jet diffusion charger. Thus, it can be seen from Fig. 3 that both large and small particles may have the same Z_p, and unambiguous size

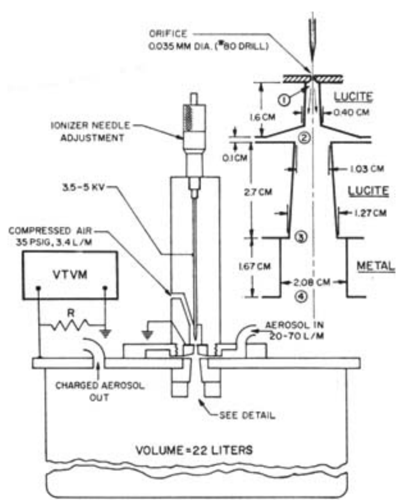

FIG. 4. Sonic jet diffusion charger.

measurement or classification is only possible if the instrument is restricted to sizes above or below the minimum Z_p.

If one is most interested in the larger particles, then one may do as LANGER *et al.* (1964) did and use strong field charging to shift the minimum Z_p to about $0.2\,\mu$ and to obtain charges proportional to about D_p^2 for $D_p > 0.3\,\mu$ (Curve A, Fig. 3).

If one is primarily interested in particles smaller than $1\,\mu$, then by using diffusion charging at moderate Nt values, the minimum Z_p may be increased to between 1 and $3\,\mu$ (Curve B, Fig. 3) and the negative slope portion of the Z_p versus D_p curve used. We took this approach because we were primarily interested in developing a technique for sizing atmospheric aerosols having relatively few particles above $1\,\mu$. Also, automatic optical counters are available for counting particles larger than $0.3\,\mu$ and cascade impactors for classifying aerosols above about $0.5\,\mu$.

The final design of the diffusion charger, Fig. 4, is an optimum design developed from a consideration of four factors. These were: (1) particle charge as a function of particle size; (2) fraction of particles smaller than about $0.05\,\mu$ that are charged; (3) loss of aerosol due to space charge; and (4) charger stability.

Operation of the charger is as follows: Negative ions generated by a sonic jet corona generator (WHITBY, 1961), are ejected downward through a conical passageway to where they mix with the aerosol entering from an annular slot. The entering aerosol is charged by diffusion as it mixes with the ions. The conical interior of the charger is made from a high resistivity plastic such as lucite to minimize loss of ions and aerosol to the cone walls. The high surface potential of the plastic helps prevent aerosol deposition in this region. At the exit of the plastic cone a short metal cylinder is located to remove some of the ions before the mixture enter the charging chamber. The total charging current is monitored by a vacuum tube voltmeter of 11 megohm input resistance connected to the charging chamber.

The sonic jet ion generator was chosen in preference to other types of ion sources because it is stable, and can easily be designed to deliver the required quantity of ions in a concentrated stream that is easily mixed with the aerosol. It is remarkably stable because the natural decay of the ion density along the axis of the ion jet makes the ion concentration beyond a cm from the orifice almost independent of the ion density at the orifice. This can easily be seen from the equation for the decay of a unipolar cloud of ions.

$$N = \frac{N_0}{4\pi e Z_i N_0 t + 1}. \tag{1}$$

The quantity $4\pi e Z_i$ has a value of about 3.6×10^{-6} for small ions. The initial ion concentration at the orifice, N_0, is on the order of 10^{10}. Therefore, N, the concentration after time, t, will be nearly independent of N_0 when Nt exceeds about 10^6—corresponding to $t < 10^{-4}$ sec, which occurs a fraction of a cm from the orifice.

The magnitude of the diffusion charge, n_p, acquired by an aerosol particle of diameter, D_p, immersed in unipolar ion cloud of density, N, for a length of time, t, has been studied by a number of investigators. Only two of these equations will be discussed here and compared with the experimental charging data.

WHITE (1951) derived the following equation for the case where $D_p \gg \lambda$, and $E = 0$.

$$n_p = \frac{D_p kT}{2e^2} \ln\left(1 + \frac{D_p \bar{c} e^2 N t}{2kT}\right). \tag{2}$$

BRICARD (1965) derived the following equation for the rate of aerosol charging for any mean free path when $E = 0$.

$$\beta = \frac{dn_p}{dt} = \frac{N\pi D_p^2 \bar{c}\,\frac{-n_p e^2}{4kT} \exp \frac{-n_p e^2}{kT(D_p/2 + \Delta)}}{n_p \frac{e^2}{kT} + \frac{\bar{c}}{16 D_i} D_p^2 \left[1 - \exp \frac{-n_p e^2}{kT(D_p/2 + \Delta)}\right]}, \tag{3}$$

where:

$$\Delta = \frac{1}{(3D_p/2)\,\lambda}\left(\frac{D_p}{2} + \lambda\right)^3 - \left(\frac{D_p^2}{4} + \lambda^2\right)^{\frac{3}{2}} - \frac{D_p}{2}.$$

The Bricard curve of n_p versus D_p shown in Fig. 5 was obtained by first integrating equation (3) with a computer to obtain the Nt corresponding to integral values of the charges and then cross plotting for a given Nt.

The experimental charging data shown in Fig. 5 was obtained as follows: Electron microscope grids placed at 5 cm intervals along the

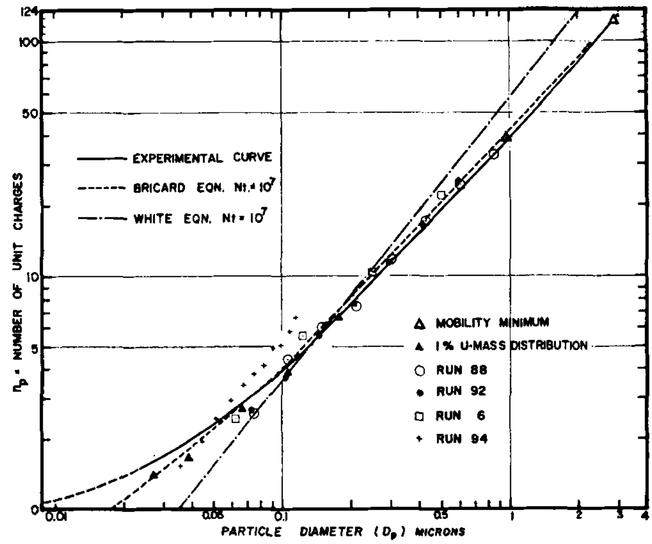

Fig. 5. Experimental and theoretical n_p versus D_p for the charger of Fig. 4. For the theoretical curves, $Z_1 = 600$ cm/sec per volt/cm, $\lambda = 1.83 \times 10^{-4}$ cm, $\delta = 1.48 \times 10^{-4}$ cm, $\bar{c} = 4.59 \times 10^4$ cm/sec, $m_1 = m_2 = 4.8 \times 10^{-23}$ gm and $D_i = 0.497$ cm²/sec. For experimental run 88, $Q_t = 127$ l/m, $Q_a = 28$ l/m, $V = 25$ KV; run 92, $Q_t = 198$ l/m, $Q_a = 57$ l/m, $V = 30$ KV; run 6, $Q_t = 127$ l/m, $Q_a = 28$ l/m, $V = 20$ KV and run 94, $Q_t = 127$ l/m, $Q_a = 28$ l/m, and $V = 8$ KV.

collector rod were used to collect spherical methylene blue particles classified from a heterodisperse aerosol. The mean mobility of each particle size was then calculated from the arithmetic mean distance of deposition, $\bar{x}$, for each particle size. The mean charge for each D_p was then calculated from equations 4 and 5 (Whitby, Jordan & Peterson, 1964).

$$n_p = \frac{3\pi\mu_g D_p Z_p}{Ce}, \quad (4)$$

$$Z_p = \frac{Q_t \ln (r_2/r_1)}{2\pi\bar{x}V} F_c, \quad (5)$$

where:

$$F_c = \frac{\frac{r_2}{2} + \left(\frac{Q_c r_2^2 + Q_a r_1^2}{4Q_t}\right)^{\frac{1}{2}} - r_1^2}{r_2^2 - r_1^2}. \quad (6)$$

The factor F_c is a correction for the fact that the aerosol particles enter the mobility analyzer, distributed across a finite width that is a function of the ratio of the aerosol flow rate, Q_a, the clean air flow, Q_c, and the radii of the inner and outer cylinder, r_1 and r_2, respectively.

The two points calculated from the mobility minimum in Fig. 5 were computed by substituting the voltage, V, at which the filter current becomes essentially equal to zero, into equation 5 to get $Z_{p\min}$ and then substituting Z_p into equation 4 with an appropriate D_p to get n_p. From Fig. 9 it is seen that the current decreases to essentially the background level at $V = 18$ KV, corresponding to a $Z_{p\min} = 0.0004$ (cm/sec)/(volt/cm).

The data points labeled "from comparison with dye mass distribution", in Fig. 5, were obtained by using the known mass distribution as calculated from electron microscope data of the dye aerosol of Fig. 11, to calculate back to n_p. The final experimental n_p vs. D_p curve of Fig. 5 was chosen taking all of the above data into account. The absolute accuracy of the experimental charge data is difficult to estimate precisely because of the complexity of the calculations. It is estimated to be about ± 20 % between 0.08 and 0.8 μ and ± 50 % for $D_p <$ 0.08 μ. Perhaps the best indication of the correctness of the epxerimental curve is that its use yields size distributions which agree with those measured by other independent methods (Figs. 10 and 11) as well as agreeing within experimental error with the direct measurements of particle charge and minimum mobility.

A precise comparison of the experimental data

TABLE 1. *Calculation of ion densities, Nt products, fraction charged and space charge losses in the sonic jet diffusion charger.*

Charger section	Air flow cm³/sec	Assumed ion loss	Ion conc. ions/cm³	Equation for Nt	Nt	Aerosol space charge loss equation	Fraction lost
1–2	58	None	3.6×10^8	—	—	—	—
2–3	534	None	3.6×10^8	$Nt_{2-3} = NL/v$	0.2×10^7	—	None
3–4	530	Eq. 1	3.6×10^8 to 5.3×10^7	$Nt_{3-4} = 1/\varkappa \ln(\varkappa N_3 t + 1)$	10^{-10}	—	Negligible
4–outlet	530	(^{a})	5.3×10^7 to 1.9×10^7 (^{b})	$Nt_{4-\text{outlet}} = \frac{2}{3} \frac{\left(\frac{3Q_{i4}}{2Z_i}\right)^{\frac{1}{2}} r_w^{\frac{3}{2}}}{Q_a e}$	1.6×10^7	(^{c})	See Table 2
					Total $= 1.8 \times 10^7$		

(^{a}) $N_{\text{outlet}} = (3Q_{i4}/2Z_i)^{\frac{1}{2}}/4\pi e r_w^{\frac{3}{2}}$. Here, Z_i was assumed equal to 600 (cm/sec)/(stat volt/cm), and r_w was taken equal to 17.3 cm, the radius of a sphere equivalent to the volume of the charging chamber.

(^{b}) Assumes $\frac{1}{2}$ of ions are lost due to entry through a hole in a grounded plane (See WHITBY, LIU & PETERSON, 1965).

(^{c}) $N_{p0}/N_{p4} = -\exp 4\pi/3Q_a\, Z_p r_w^{\frac{3}{2}}\, (3Q_i/2Z_i)^{\frac{1}{2}}$.

with either equations 2 or 3 requires that the Nt for the charger be known. Although the Nt is difficult to compute for this charger because of the complex geometry, an attempt to estimate the Nt, using the assumptions and equations of Table 1, gave a value of 1.8×10^7. However, from Fig. 5 it is seen that the theoretical curve calculated from the Bricard equation for $Nt = 10^7$ is close to the experimental curve for $D_p > 0.05\ \mu$. The difference in the curves below $0.05\ \mu$ is possibly due to the fact that the experimental average charge does not include the particles with no charge whereas the average charge computed by the Bricard equation includes the uncharged particles. Differences between the assumed and actual ion decay in the charger probably account for the difference between the calculated Nt of 1.8×10^7 and value of about 10^7 which appears to fit the experimental charging curve.

From Fig. 5 it is apparent that the Bricard equation has the same slope as the experimental curve, but that the White equation, which assumes that $\lambda \ll D_p$, does not.

The lower particle sizing and classification limit of the EPC is determined by the decreasing probability of charging with decreasing size and the increasing tendency of the small particles of high mobility to be driven to the boundaries of the system by space charge after they acquire a charge.

LIU & WHITBY (1964) have shown that the fraction charged, f, is given by:

$$f = e^{-Nt/Nt_c}, \tag{7}$$

where Nt_c is the critical Nt required for all particles to have a probability of one of acquiring a unit charge. For the theoretical calculation of f given in Table 2, Nt_c was taken equal to the Nt for a unit charge calculated from equation 3.

From an examination of the charger after a large amount of aerosol had been sampled it was determined that a negligible amount of aerosol was lost by space charge deposition between 2 and 4 and that most of the loss occurred between 4 and the aerosol outlet of the charger. The theoretical model assumed to calculate the loss of aerosol in the chamber was that of a steady state point source of ions emitted from a hole in grounded plane into a stirred aerosol. This case has been recently discussed by WHITBY, LIU & PETERSON (1965).

The fraction charged and the space charge loss were evaluated experimentally over a limited size range using electrically neutral monodisperse fluorescent dye aerosols (WHITBY, LUNDGREN & PETERSON, 1965). From fluorescence measurements of the dye caught on the collector rod, mobility analyzer after-filter, and from the aerosol concentration at the charger

TABLE 2. *Comparison of theoretical and experimental aerosol space charge loss and fraction charged.*

	$N_{p\,\text{outlet}}/N_{p4}$		f	
D_p, microns	Theoretical	Experimental	$Nt = 10^7$	Experimental
0.01	0.49		0.36	
0.015	0.72		0.62	
0.028	0.85	86.5 and 85.8	0.96	92.9 and 96.9
0.049	0.91	89.2	1.0	94.1
0.1	0.96	93.3	1.0	95.8
0.3	0.980			
1	0.985			

entrance, the experimental data of Table 2 was calculated. It is seen that the calculated and measured values of N_{p0}/Np_4 agree within experimental error but that the experimental measurements of f are somewhat lower than calculated values for the 0.049 and 0.1 μ aerosols. This disagreement is of little importance because the experimental values of f are high enough for all practical purposes.

Both N_{p0}/N_{p4} and f can be combined into a single efficiency factor, K, Fig. 6, which can be used to correct the apparent particle count of the instrument. From Fig. 6 it is seen that the useful lower particle size limit of the instrument is about 0.015 μ since the fraction charged and collected rapidly approaches zero below this size. It should be emphasized that this is a fundamental limitation of this type of instrument because if the Nt is increased to raise f, N_{p0}/N_{p4} decreases. The charger design described here represents a nearly optimum balance between these two effects.

For this instrument it is essential that the n_p versus D_p curve of the charger be independent, within reasonable limits, of the flow rate through the charger, and of the absolute ion output of the ion generator. Particle charging, Run 88, was made at 1 cfm and Run 92 at cfm but were otherwise identical. From Fig. 5 it can be seen that there is no significant difference. Also, no change was observed in the current-voltage curves on the same aerosol at 1 and 2 cfm.

Variations in the ionizer voltage from 3.5 to 5 KV and ± 10 % variation in ion generator air flow produced only a 10–20 % change in the charger current and no significant change in the aerosol current-voltage curve. It has, therefore, been concluded that the charging characteristics are independent of aerosol flow rate within the range from 1–2 cfm and of charger current within the normal variations of ionizer air flow, voltage, needle position, etc.

Mobility analyzer

The mobility analyzer shown in semi-schematic form in Fig. 7 is the result of a lengthy development program which had as its objective the design of a practical analyzer capable of laminar flow up to a Reynold's number greater than 2000, while at the same time measuring mobilities as small as 0.0004 (cm/sec)/(volt/cm). While achieving these objectives, quite a bit was learned about the requirements for maintaining laminar flow at high R_e as two different air streams are mixed. The more important "does" and "dont's" are discussed to assist anyone designing a similar unit.

Operation is as follows: Charged aerosol from the charger metered through a flowmeter having a pressure drop of 1.2 cm of water, enters the top of the analyzer column in two streams. It travels radially through two layers of 40 mesh to the inch screen to the annular space between

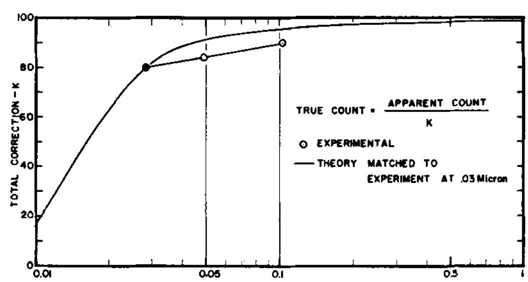

FIG. 6. Combined space charge loss and charging efficiency correction factor.

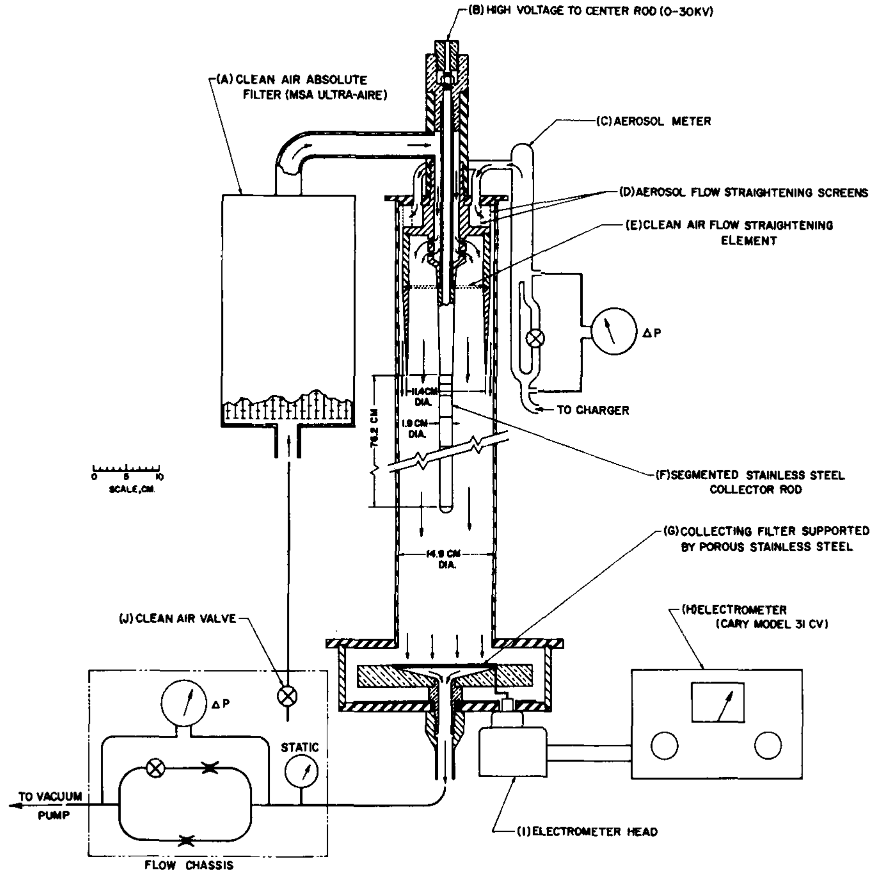

FIG. 7. Mobility analyzer.

the cone and outer cylinder, after which it flows downward to join the clean air core. Air for the clean air core first passes through a metering valve on the flow chassis, then through the absolute filter to the analyzer column where it is rectified by two layers of 240 mesh nylon screen 1 mm apart before joining the aerosol flow. The tautness, uniformity, and symmetry of these screens were found to be very critical as were the smoothness and alignment of all of the upper parts of the analyzer. This design has no asymmetric supporting structures or struts at either end of the analyzer. Struts were not used because in laminar flow the influence of a strut on the flow is proportional to its surface area whether the strut shape is streamline or not, and its influence extends much further upstream or downstream than in turbulent flow. The uniformity of the laminar flow is shown in Fig. 8 for several flow rates. It can be seen that the aerosol pattern is excellent at $Q_a = 28$ l/m, acceptable at $Q_a = 57$ l/m, but quite poor at $Q_a = 85$ l/m.

After leaving the aerosol annulus, the charged particles are subject to the cylindrical electric field between the outer grounded cylinder and the positively charged inner collecting cylinder. Those particles which miss the end of the collecting cylinder are collected by the after-filter where they give up their charge to a porous stainless steel supported glass fiber filter connected to a vibrating reed electrometer. The mobility analyzer is pivoted just below its center of gravity and connected to the filter chamber at the bottom with quick opening clamps so that it may be easily lifted and swung to a horizontal position for easy access to the collecting rod and the after filter.

All flow meter indicators, flow regulating valves, the specially designed 0–5000 volt negative and 0–30,000 volt positive power supplies, and the compressed air supply pump for the ion generator are housed in a relay rack. It was found necessary to supply regulated, dry, filtered oil-free-air from a carbon ring compressor to avoid introducing nuclei through the ion generator.

Any stable pulse free blower or vacuum pump with a capacity of 200 l/m at 2 cm Hg is satisfactory for drawing air through the unit.

Two modes of operation are possible. In the first mode, the voltage on the collector is varied in appropriate steps such as those in column 4 of Table 3 and the filter current is read to yield a voltage-current curve such as that shown in Fig. 9. The number-size distribution is then calculated from this curve directly or from the current data as shown in Table 3.

In the second operating mode, the collector voltage is set at some appropriate value, normally 15 to 30 KV, and the aerosol is classified according to electrical mobility along the length of the collector. The collector has nine stainless steel segments having lengths of 1.27, 1.91, 2.97, 4.47, 6.65, 10.2, 15.2, 16.8 and 16.8 cm which may be easily removed for analysis. Electrically neutral aerosol particles, which are mostly less than 0.02 μ in size, are collected in a sharp ring around the outer edge of the filter, similar to Fig. 8, Run 77, while any large charged particles not collected by the collector rod will be collected near the center of the filter.

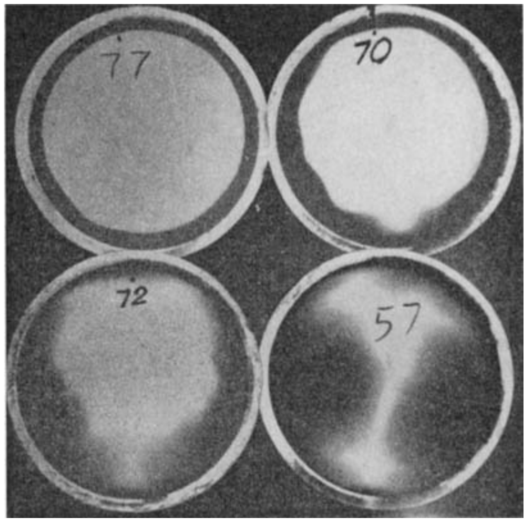

Fig. 8. Aerosol patterns on the after filter with no voltage on the collector rod: (77) $Q_a = 28$ l/m, $Q_t = 127$ l/m; (70) $Q_a = 57$ l/m, $Q_t = 198$ l/m; (72) $Q_a = 71$ l/m, $Q_t = 228$ l/m; and (57) $Q_a = 85$ l/m and 271 l/m.

TABLE 3. *Calculation of the number frequency-size distribution from the current-voltage data. Outdoor aerosol.*

$D_p - \mu$ (1)	D_{pi} (2)	n_p (3)	Collector voltage (4)	$I \times 10^{-12}$ amp. (5)	$\Delta I \times 10^{-12}$ amps. (6)	Δ No. (7)	K (8)	Δ No. c (9)	Δ No./ΔD_p (10)
.01			322	5.1					
	.0125	1.16			.49	5,593.	.32	17,479	3.50×10^6
.015			693	4.61					
	.0225	1.45			1.03	9,406.	.695	13,534	9.02×10^5
.03			1,820	3.58					
	.045	2.15			1.13	6,960.	.902	7,716	2.57×10^5
.06			4,232	2.45					
	.08	3.20			.65	2,689	.948	2,837	7.09×10^4
.10			7,207	1.80					
	.125	4.62			.8	2,292	.96	2,388	4.78×10^4
.15			9,590	1.0					
	.225	8.3			.775	1,236.	.975	1,268	8.45×10^3
.3			13,504	.225					
	.45	16.7			.160	126.5	.981	129	4.30×10^2
.6			16,505	.065					
	.8	30.0			.024	10.82	.984	11	27.5
1.0			17,884	.041					
	1.25	47.2			.016	4.95	.990	5	10
1.5			19,005	.025					

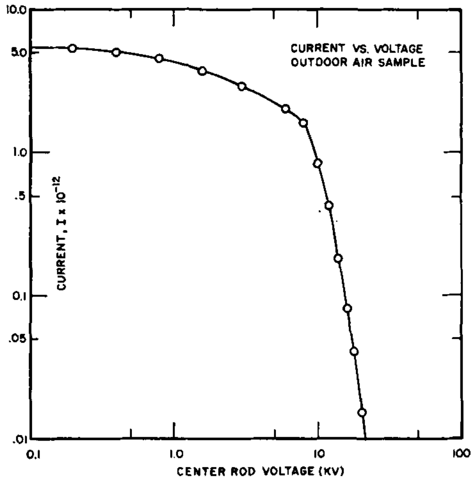

FIG. 9. Current-voltage curve for the outdoor aerosol of Fig. 10.

Thus, the very large and very small particles may be analyzed separately by cutting the filter at the appropriate radius.

Sensors

Two particle sensors at the end of the mobility analyzer tube have been evaluated. The most satisfactory is a Cary Model 31 vibrating reed electrometer using 10^{11} ohm resistors across the input. A General Electric nuclei counter has been tried but was not satisfactory because under most atmospheric conditions the number of particles in the size range between the cutoffs of the EPC and nuclei counter fluctuates rapidly. This decreases the sizing accuracy below an acceptible level.

Experimental

In addition to the measurement of the particle charge versus particle size described earlier in connection with the charger description, the performance of the EPC has been studied in a number of other ways as described below.

Background Counts

With an absolute filter on the aerosol inlet, the charger operating at 3.6 KV and 30 KV on the collector, the background current was about 10^{-14} amps with a total flow of 130 l/m.

Since it has been reported that a corona at a needle point may produce condensation nuclei, a series of experiments were conducted in which the after-filter and its support plate were removed and the nuclei count at the mobility analyzer exit was measured while the EPC was sampling particle free air. The only experiments in which the nuclei count rose above the lower sensitivity limit of the nuclei counter (10 to 20 nuclei/cm^3) were those in which the ion generator voltage was increased from the normal voltage of 3.5 KV to 5 KV. For about three minutes after the increase, the count rose to 40/cm^3 and then fell to about 15/cm^3. From these experiments we have concluded that the sonic jet ion generator does not produce a significant number of nuclei in normal operation.

Size distribution measurements with the counter system

Described below are several size distribution and classification measurements made with a particle counting system consisting of a General Electric nuclei counter, the EPC, and a Royco Model PC 200 A optical counter. The sizing range of the Royco is 0.3 to 10 μ, and the EPC is 0.015 to 1 μ. Since the nuclei counter gives the total number of all sizes of particles, the difference between the EPC and CNC count can be assigned to the 0.002 to 0.015 μ size range.

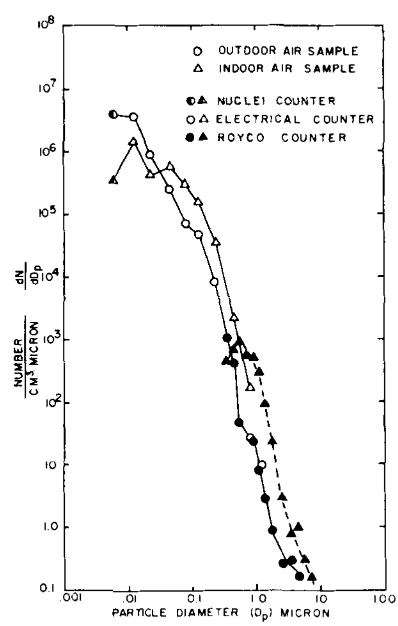

FIG. 10. Size distributions of an outside and a laboratory aerosol.

TABLE 4. *Calculation of the cumulative mass-size distribution of a 1 % uranine dye aerosol.*

X, cm (1)	Uranine mass μ gm (2)	Z_p (3)	$D_p-\mu$ (4)	$D_{pi}-\mu$ (5)	K (6)	Uranine mass μ gm (corrected) (7)	% Mass < D_p (8)
0							
	0						
1.27		.0224	.01				
	.0184			.013	.345	.0533	
3.175		.00898	.016				.235
	.0424			.0205	.65	.0652	
6.147		.00464	.025				.522
	.234			.0325	.85	.275	
10.617		.00268	.04				1.73
	1.723			.05	.915	1.88	
17.27		.00165	.06				10.02
	8.023			.08	.95	8.445	
27.43		.00104	.1				47.22
	8.691			.145	.965	9.006	
42.67		.000668	.19				86.89
	2.57			.295	.98	2.62	
59.44		.000479	.40				98.44
	.35			.85	.986	.355	
76.2		.000374	1.3				100.0 %
						Total 22.7	

Thus, the three instruments operated together are capable of measuring the number-size distribution of an aerosol from 0.002 to 10 μ.

Fig. 10 shows the number-size distributions of an aerosol sampled outside the laboratory windows and one sampled inside the laboratory. The procedure for calculating the number distribution of the outdoor aerosol from the EPC data is shown in Table 3, and the distributions are plotted in Fig. 10. Column 3 is obtained from Fig. 5. The currents in column 5 may be obtained either by taking current readings with the collector set at the voltages of column 4 or from a current-voltage curve constructed from currents read at a series of arbitrary voltage settings. The number concentration in each size range, ΔN in column 7, is calculated from equation 8.

$$\Delta N = \frac{\Delta I}{e n_p Q_a}. \tag{8}$$

The ΔN_c is obtained by dividing ΔN by K, the analyzer efficiency, and, finally, the number frequency corrected for the size interval is computed in column 10.

Several observations may be made from Fig. 10. For the outdoor aerosol it will be noted that the EPC and Royco agree quite well in the size range where they overlap. However, for the indoor aerosol the Royco shows a mode at about 0.5 μ and a higher count in the size range where they overlap. From calculations and experi-

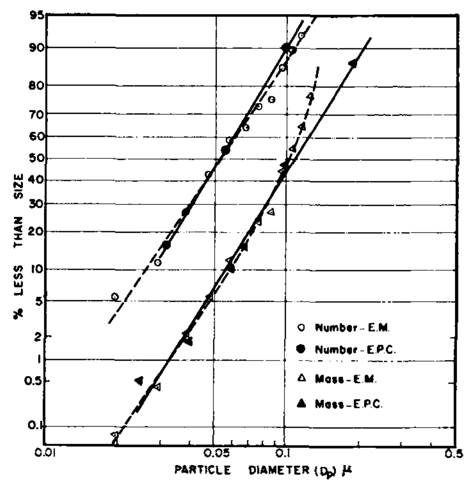

FIG. 11. Number and mass distributions of atomizer-impactor generated 1 % uranine aerosols sized by electron microscopy (EM) and electrical particle counter (EPC). Collector voltage = 20 KV; Aerosol flow = 28 l/m.

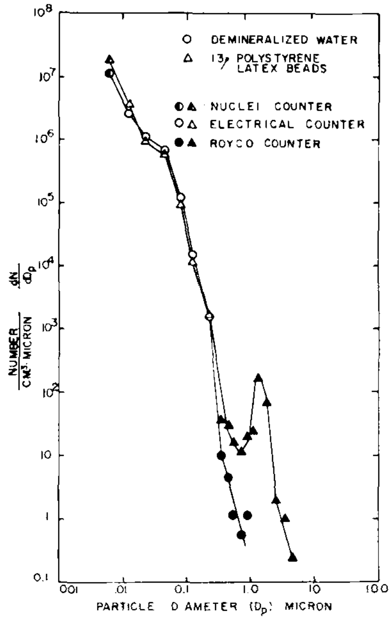

FIG. 12. Size distribution of the residue from the atomization of distilled water and distilled water suspension of 1.3 μ polystyrene latex.

ments to be discussed in a future paper it is believed that this is an apparent mode and the size shift is due to scattering from the large number of particles less than 0.3 μ in size. The mode in the indoor aerosol distribution at 0.04 μ was apparently caused by oil aerosol from a vacuum pump operating in the laboratory.

An atomizer-impactor generated aerosol having accurately known number and weight-size

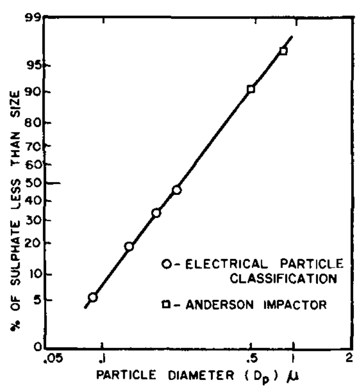

FIG. 13. Sulfate mass distribution classified from 24-hour sample of outdoor aerosol March 26, 1965. Weather was clear, cold and with low wind velocity.

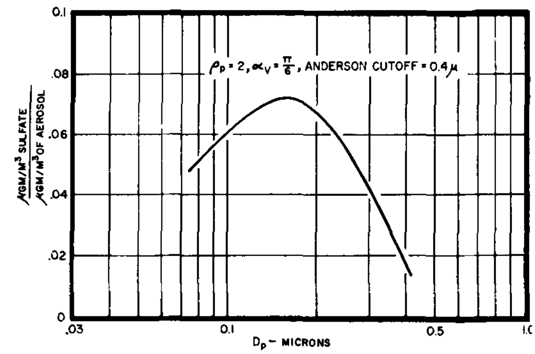

FIG. 14. Fraction of aerosol consisting of sulfate computed from number distribution and the sulfate mass distribution of Fig. 13.

distributions was sized with the EPC and the total aerosol count obtained with the CNC counter. The number-size distribution was measured electrically by the same procedure as that described above for the airborne dusts. The weight-size distribution was obtained by fluorometric analysis of the amount of dye on each collector segment and the mass distribution computed as shown in Table 4. Results are shown in Fig. 11. It will be noted that agreement with both the number and weight distributions is good. Also, the total number concentration of 40,450 measured by the EPC agrees well with the value of 40,000 measured by the CNC counter.

Fig. 12 shows the size distribution of the aerosol from a small glass vaponifrin atomizer used to generate at 1.3 μ polystyrene latex aerosol from a distilled water suspension and the aerosol generated from the distilled water alone. It will be noted that the distribution below 0.2 μ is practically the same with and without the latex. It is obvious that the large number of submicron aerosol particles present with the latex would have to be taken into account if such an aerosol was used for nucleation experiments or for the calibration of optical counters when the total light scattered by these particles is an appreciable fraction of the magnitude of the light scattered by a single particle in the counting range.

On March 26, 1965, a 24-hour sample of outdoor aerosol was classified and analyzed for sulfate by the Laboratory of Physical Sciences, USPHS Div. of Air Pollution, Cincinnati, Ohio, to determine the feasibility of using the EPC

TABLE 5. *Practical particle sizing and classification characteristics for the EPC.*

Characteristic	Aerosol flow, l/m 28	57
Min. D_p	0.015 μ	0.015 μ
Max. D_p electric sizing[a]	1.2	0.8
Max. D_p mass classification	0.6	0.4
σ_g number classification	1.3 – 2.	
σ_g mass classification	1.3 – 1.6	1.3 – 1.6

[a] For natural aerosols having size distributions and concentrations similar to Fig. 10.

in series with a cascade impactor for analysis of atmospheric pollutants. An Anderson impactor was used in series ahead of the EPC. At the sampling rate of 28 l/m the lower cutoff of the Anderson was estimated to be 0.4 μ. The data was corrected with an 8 hour blank run. Total sulfate collected was 474 μ gm.

The cumulative % of sulfate less than size is shown in Fig. 13, and the fraction of the total aerosol represented by the sulfate is shown in Fig. 14. This latter curve was computed from the number distribution of the aerosol determined electrically with the EPC, the total mass of sulfate and the sulfate mass distribution.

Because this data is the result of only a single run, not too much significance should be attached to these results. However, it does suggest that the EPC-impactor combination should be useful for the classification and analysis of air pollutants.

Sizing and classification limits

From the analysis of the electron micrographs used in the determination of the n_p versus D_p curve and from comparisons such as those shown in Figs. 10 and 11, the sizing and classification characteristics summarized in Table 5 have been determined.

The smallest particle that may be collected with useful efficiency is about 0.015 μ for reasons discussed in the section on the charger.

The maximum size particle which can be sized electrically or classified depends on the aerosol characteristics, the accuracy required and the EPC operating conditions. From Fig. 3, Curve B, it will be noted that the absolute slope of the Z_p versus D_p curve decreases from 1 at 0.3 μ to 0.156 at 1 μ. This decrease in slope, coupled with the statistical nature of the charging process, determines the maximum D_p which will be resolved with acceptable accuracy. The maximum D_p is about 1 μ for electrical sizing but only about 0.5 μ for classification because the fact that n_p is approximately proportional to D_p means that the measured current per particle and, hence, the sensitivity is greater for larger particles than for small. When using the instrument as a classifier, it is recommended that the deposit collected at collector lengths greater than those corresponding to 0.6 μ at 28 l/m and 0.4 μ at 57 l/m be pooled because of the decreased resolutions for larger sizes. A cascade impactor may be used ahead of the EPC to classify the larger particles.

REFERENCES

BRICARD, J., 1965, Action of Radioactivity and of Pollution upon Parameters of Atmospheric Electricity. S. C. Coroniti, Editor, Elsevier Publ. Co, Amsterdam.

LANGER, G., PIERRARD, J., and YAMATE, G., 1964, Further development of an electrostatic classifier for submicron airborne particles. *Intl. J. of Air Water Pollution*, **8**, pp. 167–176.

LIU, B. Y. H., and WHITBY, K. T., 1964, Experimental study of particle charging at low pressures. Presented at AEC Conf. on Radioactive Fallout from Nuclear Weapons Tests, Germantown, Md., Nov. 3–6, 1964. To be published in *Proceedings*.

RANDALL, J. M., and KELLER, J. D., 1965, Electrooptical aerosol counter instrumentation. Presented at the 1965 AIHA Conference, Houston, Texas, May 3–7.

ROHMAN, H., 1923, *Physik*, **17**, p. 18.

SKALA, G. F., 1963, A new instrument for the continuous measurement of condensation nuclei. *Anal. Chem.*, **35**, p. 702.

THOMAS, A. C., BIRD, A. N., COLLINS, R. H., and RICE, P. C., 1960, A Portable Photoelectric Aerosol Counter and Particle Size Analyzer. Instr. Soc. of Am. Preprint No. 23-SF60.

WHITE, H. J., 1951, Particle charging in electrostatic precipitation. *AIEE Trans.*, **70**, pp. 1186–1191.

WHITBY, K. T., 1961, Generator for producing high concentrations of small ions. *Rev. Sci. Inst.*, **32**, 351–55.

WHITBY, K. T., JORDAN, R. C., and PETERSON, C. M., 1964, Development of a Particle Counter System and Development of a Technique for Studying the Charge on an Evaporating Drop. Particle Laboratory Report No. 80, Mechanical

Engr. Dept., Univ. of Minnesota to USPHS, June, 1964.

Whitby, K. T., Liu, B. Y. H., and Peterson, C. M., 1965, Charging and decay of monodisperse aerosols in the presence of unipolar ion sources. *J. Coll. Sci.*, **20**, p. 585.

Whitby, K. T., Lundgren, D. A., and Peterson, C. M., 1965, Homogeneous aerosol generators. *Intl. J. Air Water Poll.*, **9**, pp. 263–77.

Whitby, K. T., and Vomela, R. A., 1965, Evaluation of Optical Particle Counters. Particle Laboratory Report No. 86, Mechanical Engr. Dept, Univ. of Minnesota, to USPHS, May, 1965.

Zinky, W. R., 1962, A new tool for air pollution control, the aerosol paricle counter. *APCA J.* **12**, pp. 578–83.

ИЗМЕРИТЕЛЬНАЯ СИСТЕМА ДЛЯ СЧЕТА И РАСПРЕДЕЛЕНИЯ ПО РАЗМЕРАМ ЭЛЕКТРИЧЕСКИ ЗАРЯЖЕННЫХ ЧАСТИЧЕК АЭРОЗОЛЯ В ДИАПАЗОНЕ РАЗМЕРОВ ОТ 0,015 ДО 1,0 μ.

Описана система для подсчета и определения размеров заряженных частиц со следующими характеристиками.

1. Диапазон измерений от 0,015 до 1,2 μ.
2. Классификация частиц по размерам в диапазоне от 0,015 до 0,6 μ при скорости аэрозолей в 28 л/мин.
3. Своеобразный униполярный диффузионный заряжатель, который является устойчивым и контролируемым в работе и позволяет работать в близи от оптимального режима заряжания частиц.
4. Мобильный анализатор подвижности позволяет классифицировать частицы с подвижностью от 0,01 до 0,0002 см^2/сек. при скорости потока аэрозолей вплоть до 57 л/мин. Своеобразием этого анализатора является наличие фильтра в кормовом конце токоснимателя. Такое разделение собирающего электрода и токоснимателя позволяет использовать на коллекторе напряжение до 30 кв, при поддерживающем фоновом тоне ниже 10–14 ам.
5. На ряду с описываемым здесь полуавтоматическим прибором, осуществлен практически полностью так же и его автоматический вариант. Использование его вместе с автоматическим CN и оптическим счетчиком должно позволить непрерывно автоматически определять распределение частиц по размерам в области 0,01–10 μ.